

Required bracing stiffness on lateral buckling strength for H-shaped beams with bracings

Y. Kimura & Y. Yoshino
Tohoku University, Japan

Abstract

Lateral bracings are usually set to upper flanges of H-shaped beams in moment resisting frames, and then the stress of the braced flange may become tensile. If the bracings are connected to the tensile flange of H-shaped beams, its lateral buckling strength is more increased than that without bracing. The bracing connected to a tensile flange must restrain torsion to increase the lateral buckling strength of the beams. In this paper, the elastic lateral buckling load of H-shaped beams is developed with the energy method, and the relationship between the lateral buckling load and bracing rigidity is clarified. Bracing rigidities are lateral and rotational rigidities. The required bracing rigidity is suggested from two equations of the elastic lateral buckling load. Next, large deformation analyses are performed using ABAQUS with version 6.8, and the elasto-plastic lateral buckling behaviour for H-shaped beams with lateral and rotational bracings is presented. Also the buckling load is related with lateral and rotational bracings. Finally, the lateral buckling load for H-shaped beams with the required bracing rigidity is estimated with the modified equivalent slenderness ratio, and the elasto-plastic buckling stress is compared with the buckling curve for the Japanese standard code

Keywords: lateral buckling H-shaped beam, bracing stiffness.

1 Introduction

Lateral buckling of an H-shaped beam is considered as flexural buckling of its compressive flange, so that in the Japanese design code, the braces for the beams are laterally supported to be set up on their compressive flanges or both flanges. On the other hand, the braces are jointed on upper flanges of beams in the real structures, and the stress on the upper flange at the bracing point may become



tensile by the combination of the dead load and lateral seismic load. Therefore, when braces are jointed on upper flange to beams, the upper flange is braced laterally, whereas the other flange is free to displace. Therefore, the beams might undergo lateral buckling deformation of under flanges with torsion.

This paper develops the elastic buckling load for H-shaped beams with lateral and rotational braces on the upper flanges, and suggests the required bracing stiffness to restrain the buckling deformation of H-shaped beams at the bracing points. In additions, it clarifies the elasto-plastic buckling behavior for these beams, and evaluates the elasto-plastic lateral buckling stress of these beams using modified equivalent slenderness ratio.

2 Elastic buckling load for H-shaped beams with bracings subjected to pure bending moment

2.1 Development of elastic buckling load for H-shaped beams with bracings subjected to pure bending moment

In this section, the elastic buckling load for H-shaped beams with bracings is obtained using the energy method and the eigenvalue analyses. When H-shaped beams with braces are subjected to equal and opposite couples of bending moment, they are buckled laterally and torsionally. The potential energy U is expressed as the following (Bleich [1], Kimura and Yoshino [2]).

$$U = \frac{1}{2} \int_0^l \left[EI_f u_1''^2 + EI_f u_2''^2 + GK \beta_0'^2 - P_1 u_1'^2 - P_2 u_2'^2 \right] dz + \frac{1}{2} K_u u_0^2 \Big|_{z=\frac{l}{2}} + \frac{1}{2} K_\beta \beta_0^2 \Big|_{z=\frac{l}{2}} \quad (1)$$

where, EI_f is the flexural rigidity of each flange for H-shaped beam, GK is the torsional rigidity of H-section. K_u is the lateral rigidity of the brace and K_β is the rotational rigidity of the brace. l is the length of H-shaped members. P_i and u_i are the compression load and the lateral deformation at the center of the flanges, u_0 is the lateral displacement at the brace point. β is the torsional angle. The boundary condition is simple support to strong and weak axes. The lateral deformation of member and web deformation are expressed as a function of the sine curves in the following.

$$u_1 = a_1 \sin \frac{\pi}{l} z + a_2 \sin \frac{2\pi}{l} z, \quad u_2 = b_1 \sin \frac{\pi}{l} z + b_2 \sin \frac{2\pi}{l} z \quad (2)$$

It is also assumed that braces are set up at upper flange, so u_0 is equal to u_1 . Lateral displacement of the bracing, u_0 , and torsional angle at the bracing point of beam, β_0 , is expressed with the lateral deformation of flanges, u_1 and u_2 as the following, respectively.

$$u_0 = u_1 \quad (3)$$

$$\beta_0 = \frac{u_2 - u_1}{d} \quad (4)$$



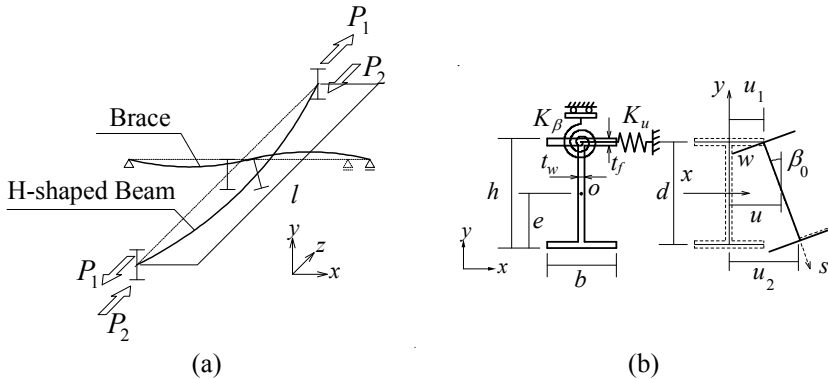


Figure 1: Lateral buckling deformation of H-Shaped beam with bracing on upper flange. (a) Lateral buckling of H-shaped beam; (b) Buckling deformation of H-shaped beam at bracing point.

Substituting Eqs. (2) to (4) for Eq. (1), the buckling load, P_{cr} , is obtained.

$$P_{cr} = \frac{K_u}{l} \left(\frac{l}{\pi} \right)^2 + \sqrt{\left\{ \frac{K_u}{l} \left(\frac{l}{\pi} \right)^2 \right\}^2 + \left\{ EI_f \left(\frac{\pi}{l} \right)^2 + \frac{GK}{d^2} + \frac{2K_\beta}{ld^2} \left(\frac{l}{\pi} \right)^2 \right\}^2} \quad (5)$$

$$+ \frac{2K_u}{l} \left(\frac{l}{\pi} \right)^2 \left\{ EI_f \left(\frac{\pi}{l} \right)^2 + \frac{GK}{d^2} + \frac{2K_\beta}{ld^2} \left(\frac{l}{\pi} \right)^2 \right\} - \left\{ \frac{GK}{d^2} + \frac{2K_\beta}{ld^2} \left(\frac{l}{\pi} \right)^2 \right\}^2$$

$$P_{cr} = -\frac{K_u}{l} \left(\frac{l}{\pi} \right)^2 + \sqrt{\left\{ \frac{K_u}{l} \left(\frac{l}{\pi} \right)^2 \right\}^2 + \left\{ EI_f \left(\frac{\pi}{l} \right)^2 + \frac{GK}{d^2} + \frac{2K_\beta}{ld^2} \left(\frac{l}{\pi} \right)^2 \right\}^2} \quad (6)$$

$$+ \frac{2K_u}{l} \left(\frac{l}{\pi} \right)^2 \left\{ EI_f \left(\frac{\pi}{l} \right)^2 + \frac{GK}{d^2} + \frac{2K_\beta}{ld^2} \left(\frac{l}{\pi} \right)^2 \right\} - \left\{ \frac{GK}{d^2} + \frac{2K_\beta}{ld^2} \left(\frac{l}{\pi} \right)^2 \right\}^2$$

Eqs. (5) and (6) are the equation for the lateral buckling load of H-shaped beam with bracing on compressive flange and that on tensile flange. For these equations, the lateral deformation of H-shaped beam at the bracing point is assumed to occur.

On the other hand, when the lateral deformation of H-shaped beam is restrained at the bracing point, Eq. (7) is developed from Eq. (1) in the condition of $a_1=b_1=0$.

$$P_{cr} = \sqrt{8 \left[EI_f \left(\frac{\pi}{l} \right)^2 \left\{ 2EI_f \left(\frac{\pi}{l} \right)^2 + \frac{GK}{d^2} \right\} \right]} \quad (7)$$

The smaller value of P_{cr} obtained from Eqs. (5) and (7) is useful as the lateral buckling load for H-shaped beams with bracing on the compressive flange. Similarly, the smaller value of P_{cr} obtained from Eqs. (6) and (7) is useful as the lateral buckling load for H-shaped beams with bracing on the tensile flange. Type A and Type B represent the beam with bracing on the compressive

flange and that with bracing on the tensile flange, respectively. The lateral buckling moment, M_{cr} , is calculated from P_{cr} obtained from Eqs. (5)–(7) multiplied by the distance of both flanges, d .

2.2 Effect of bracing stiffness on elastic buckling load for H-shaped beams with bracings subjected to pure bending moment

Fig. 2 presents the numerical analysis model for H-shaped beams with bracing on upper flange. ABAQUS with version 6.8 is used as numerical analyses program. The H-shaped beam and vertical stiffeners at the bracing point consists of four node shell elements, and the bracings are replaced on the lateral and rotational springs. The boundary condition is simple support to strong and weak axes. Herein, cross-sectional shapes of three kinds are adopted as shown in Table 1. Then each cross-sectional shape is selected as the ratio of flange width to web depth, $b/h=0.5, 0.77$, respectively. For these examinations, a 0–200 lateral rigidity ratio $K_u/(EI_y/l^3)$ and a 0–15 rotational rigidity ratio $K_\beta/(GK_\beta/d)$ are adopted.

Table 1: Cross sectional shape of H-shaped beams.

| b/h | h | b | t_w | t_f |
|-------|-----|-----|-------|-------|
| 0.5 | 500 | 250 | 9 | 16 |
| 0.77 | 390 | 300 | 10 | 16 |

(mm)

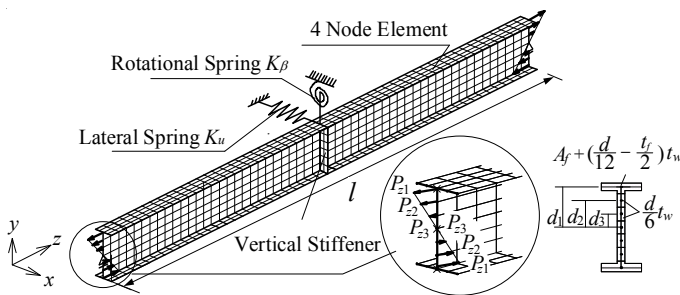


Figure 2: Numerical analysis model.

Fig. 3 presents the relation between the elastic buckling stress, σ_{cr} , for H-shaped beams with bracing on upper flange and slenderness ratio, λ . The curves show the buckling stress, P_{cr}/A , obtained from Eqs. (5)–(7). The symbols show the eigenvalue analyses results. The parameters are $b/h=0.5$, $K_u/(EI_y/l^3)=200$ and $K_\beta/(GK_\beta/d)=5$. The buckling curves obtained from Eqs. (5)–(7) and the symbols of the eigenvalue analyses results are very fitting well, so that Eqs. (5)–(7) can be applied to estimate the elastic buckling stress of H-shaped beams with bracings. The black and grey curves show the buckling stress for type A and type B,



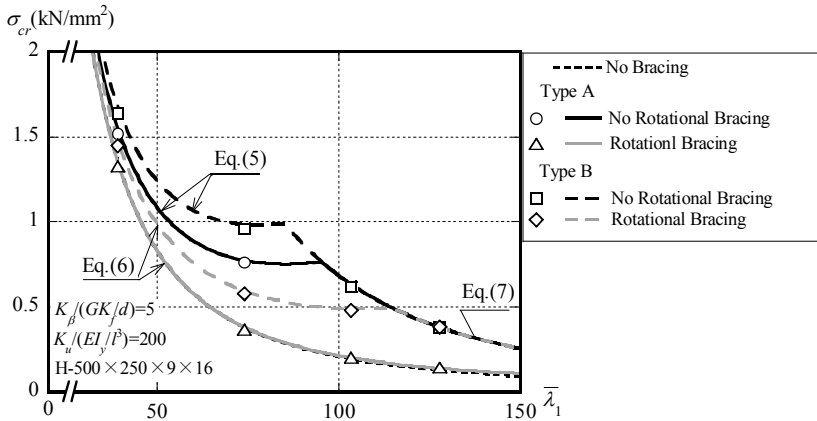


Figure 3: Lateral buckling elastic stress of H-shaped beams with bracing on upper flange.

respectively. In additions, the solid and broken curves show the buckling stress for beams with the lateral brace, and that with the lateral and rotational braces, respectively. The buckling stress for type B with the lateral brace is almost equal to that for the beams with no brace. For type B, the lateral brace is not effective to increase the buckling stress, and for type B with the lateral and rotational braces, the buckling stress increases about twice more than that for with no brace at $\lambda=100$. The lateral buckling stress for type B with the lateral and rotational braces obtained from Eq. (6) becomes that for perfect support at the bracing point obtained from Eq. (7) when λ is more than 120. On the other hand, the bucking stress for type A increases more than that for type B. The buckling stress for Type A with the lateral and rotational braces obtained from Eq. (7) is applied when λ is more than 80.

Fig. 4(a) shows the relation between the ratio of the buckling moment, M_{cr}/M_{cr0} , and the lateral rigidity ratio, $K_u/(EI_y/l^3)$. In fact, Fig. 4(b) shows the relation between the ratio of the lateral buckling moment, M_{cr}/M_{cr0} , and the rotational rigidity ratio, $K_\beta/(GK_f/d)$. Fig. 4(a) shows the effect of the lateral rigidity on the lateral buckling moment and for type A and type B. Fig. 4(b) shows the effect of the rotational rigidity on the lateral buckling moment for type B with the lateral and rotational braces, where $M_{cr}/M_{cr0}=3.3$ represents the upper bound for the ratio of lateral buckling moment. The dots in Fig. 4(a) and 4(b) are the points to change from the lateral buckling with the lateral deformation at the bracing point to the lateral buckling for perfect support at the bracing point. As presented in Fig. 4, the curve for type A reaches 3.3, even though the rotational rigidity is equal to 0. For type B, the curve for $K_\beta/(GK_f/d)=8$ reaches 3.3, and the curves for $K_\beta/(GK_f/d)=0$ and 5 does not reach 3.3, even though the rotational rigidity ratio becomes larger. In Fig. 4(b), the larger the rotational rigidity becomes, the larger M_{cr}/M_{cr0} becomes. As the rotational rigidity ratio becomes larger, the lateral rigidity ratio at $M_{cr}/M_{cr0}=3.3$ becomes smaller.

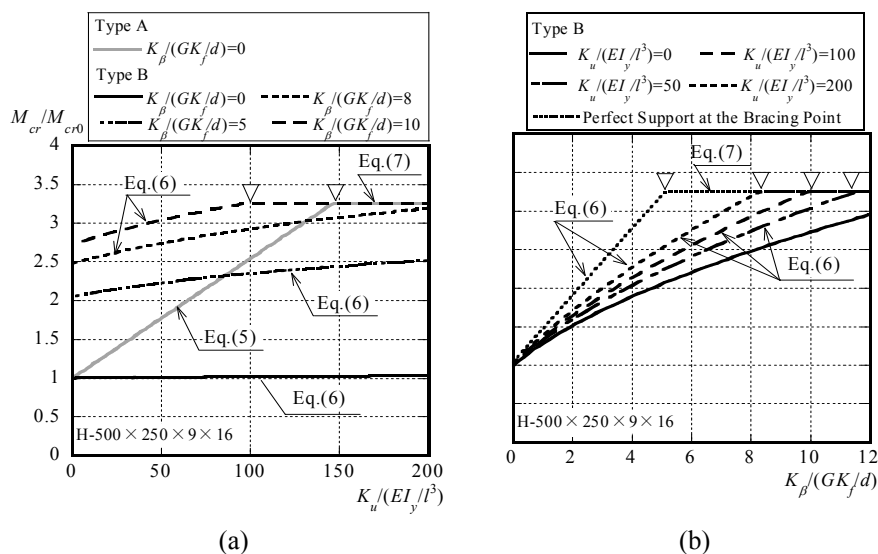


Figure 4: Relation between ratio of buckling load and bracing rigidity. (a) Effect of lateral stiffness; (b) Effect of rotational stiffness.

3 Estimation of elastic-plastic buckling stress for H-shaped beams with bracings subjected to pure bending moment

3.1 Elasto-plastic buckling behaviour for H-shaped beams with bracings

Fig. 5 shows the elasto-plastic buckling behavior for H-shaped beams with braces at the upper flanges of beams. The parameter in Fig. 5 is the lateral bracing type such as no bracing, a bracing at compressive flange (type A), and at tensile flange (type B). Figs. 5(a)–5(d) present the bending moment M/M_y , the lateral displacement u/l , the torsional angle β , and the lateral buckling mode at twice the yield rotation $2\theta/\theta_y$. The symbols u , and β in Figs. 5(b)–5(c) are the displacement at the center of members. In Figs. 5(a)–5(d), maximum bending moment for the beams with lateral bracings are larger than that with no bracing. For type A with the lateral brace and type B with the lateral and rotational braces, the maximum bending moment is identical. The rotational brace is effective to increase the maximum bending moment. In Figs. 5(b) and 5(c), u and β for type A with the lateral brace and type B with lateral and rotational braces, are more restrained than that with no bracing and type B with the lateral bracing. In Fig. 5(d), the buckling modes for the beams with no bracing and with lateral bracing at the tensile flange are almost identical and the maximum displacement occurs at the center of the beams. The deformation of the other beams is restrained at the center.

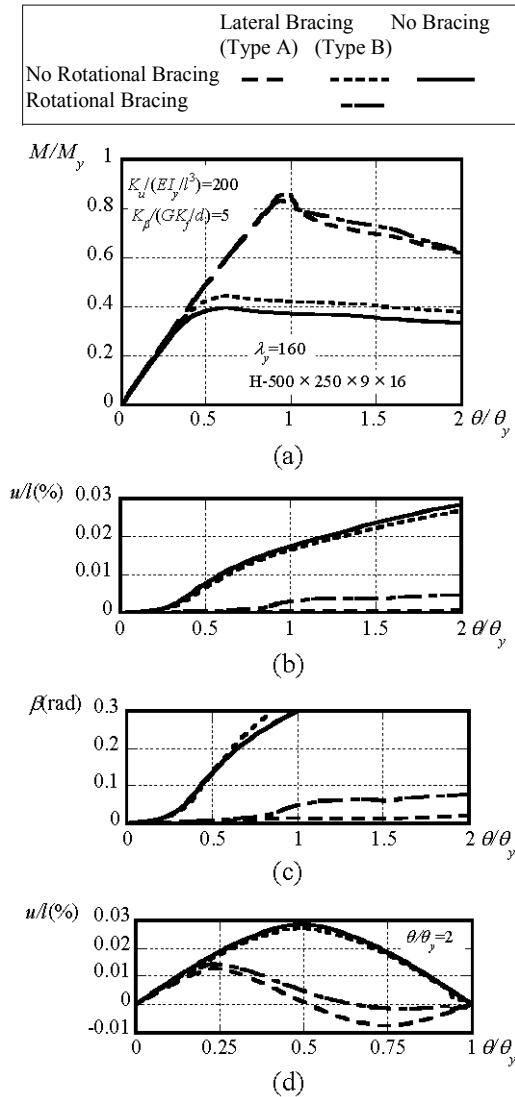


Figure 5: Lateral buckling behavior of H-shaped beams with lateral bracings. (a) Relation between bending moment and rotation; (b) Relation between lateral deformation and rotation; (c) Relation between torsion and rotation; and (d) buckling deformation of H-shaped beams.

3.2 Estimation of elasto-plastic buckling stress for H-shaped beams with bracings

Fig. 6 portrays the relation between the elasto-plastic buckling stress σ_{cr}/σ_y for H-shaped beams with braces and modified equivalent slenderness ratio λ_c . In fact, λ_c is shown as the following in the Japanese design code (AIJ [3]).

$$\lambda_c = \sqrt{P_y / P_{cr}} \quad (8)$$

In that equation, P_y is the yield load; P_{cr} is Euler's buckling load. When H-shaped beams are braced at the flanges of beams, Euler's buckling load in Eq. (8) is replaced on the buckling load obtained from Eqs. (5)–(7). This equivalent slenderness ratio is called the modified equivalent slenderness ratio. These curves in Fig. 6 are the buckling stress curves for Japanese design codes (AIJ [3, 4]), and the tangent line of Euler's buckling curve from $\sigma_{cr}/\sigma_y=0.6$. The symbols show results of numerical analyses, which constantly exceed the curve for the Japanese design code equation (AIJ [3]), distributed as the upper-bound for the tangent line of $\sigma_{cr}/\sigma_y=0.6$. Consequently, the elasto-plastic buckling stress for H-shaped beams with braces can be evaluated approximately by the buckling curves in Japanese design codes using the modified equivalent slenderness ratio.

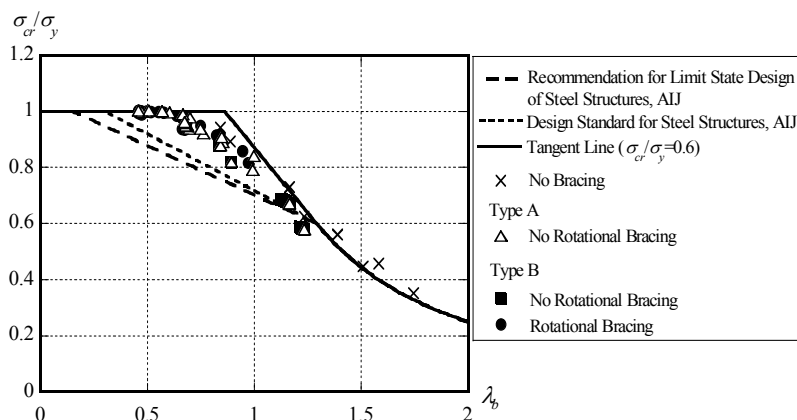


Figure 6: Lateral buckling stress of H-shaped beams with braces.

4 Conclusions

This paper evaluated the effect of the lateral and rotational braces on lateral buckling stress for H-shaped beams. Results show the following.

1. The elastic buckling load for H-shaped beams with the lateral and rotational braces is obtained from Eqs. (5)–(7). When braces are supported on compressive flange of beams, the smaller value of P_{cr} obtained from

Eqs. (5) and (7) is applicable to the elastic buckling load for these members. When braces are supported on tensile flange of beams, the smaller value of P_{cr} obtained from Eqs. (6) and (7) is applicable to the elastic buckling load for these members.

2. The approximate elasto-plastic buckling stress for H-shaped beams with the lateral and rotational braces can be estimated using the equations in the Japanese design codes with the modified equivalent slenderness ratio in Eq. (8).

References

- [1] Bleich, F. (1952). Buckling Strength of Metal Structures, McGraw-Hill Book Co., 142-147.
- [2] Kimura, Y. and Yoshino, Y. (2011). Required Bracing Capacity on Lateral Buckling Strength for H-shaped beams with bracings, AIJ. 76, 670, 2143-2152 (in Japanese).
- [3] Architectural Institute of Japan, AIJ (1998). Recommendation for Limit State Design of Steel Structures (in Japanese).
- [4] Architectural Institute of Japan, AIJ (2005). Design Standard for Steel Structures (in Japanese).

